Cascade energy transfer versus charge separation in ladder-type oligo(*p*-phenylene)/ZnO hybrid structures for light-emitting applications

F. Bianchi,[1] S. Sadofev,[1] R. Schlesinger,[1] B. Kobin,[2] S. Hecht,[2] N. Koch,[1] F. Henneberger,[1] and S. Blumstengel[1,a)]
[1]*Institut für Physik & IRIS Adlershof, Humboldt-Universität zu Berlin, Newtonstr. 15, 12489 Berlin, Germany*
[2]*Institut für Chemie & IRIS Adlershof, Humboldt-Universität zu Berlin, Brook-Taylor-Str. 2, 12489 Berlin, Germany*

(Received 31 October 2014; accepted 24 November 2014; published online 8 December 2014)

Usability of inorganic/organic semiconductor hybrid structures for light-emitting applications can be intrinsically limited by an unfavorable interfacial energy level alignment causing charge separation and nonradiative deactivation. Introducing cascaded energy transfer funneling away the excitation energy from the interface by transfer to a secondary acceptor molecule enables us to overcome this issue. We demonstrate a substantial recovery of the light output along with high inorganic-to-organic exciton conversion rates up to room temperature. © *2014 AIP Publishing LLC*. [http://dx.doi.org/10.1063/1.4903517]

Hybrid inorganic/organic semiconductor structures (HIOS) are promising candidates for achieving improved or even new opto-electronic functionalities. Control of the electronic coupling at the heterointerface is a crucial aspect in this context. In HIOS comprised of a ZnO quantum well (QW) and an adjacent organic layer, efficient conversion of Wannier excitons into Frenkel excitons via Förster-type resonant energy transfer (FRET) has been demonstrated.[1,2] Similar observations were made for GaN, InGaN, or GaAS as donor material.[3–5] In this way, the difficulty of injecting high carrier densities directly into the organic material can be circumvented. Hybrid light emitters based on this concept will combine the exceedingly high electrical injection rates of inorganic semiconductors with the unsurpassed radiation output of molecular systems. For achieving truly superior operation in comparison to the single components, the inorganic/organic excitonic coupling must be very efficient and loss channels of the excitation energy at the hybrid interface rendered inactive. To meet the first challenge, we introduce ladder-type oligo(*p*-phenylenes) (LOPPs) as efficient FRET partners for ZnO.[6–8] Due to their rigid planar geometry, LOPPs exhibit weakly Stokes-shifted absorption and emission spectra featuring well-resolved vibronic progressions. Their absorption coefficients are much larger than those of the respective oligo(*p*-phenylenes) with non-rigidified backbone and the LOPPs' fluorescence yield reaches unity in solution.[6] Moreover, the exciton transition of ladder-type quarterphenyl (L4P) and its spiro-derivatives is almost in resonance with that of ZnO. However, despite all these favorable features, an intrinsic loss channel of the excitation energy might be present due to an unfavorable energy level alignment between the frontier molecular levels and the band edges of the inorganic semiconductor at the hybrid interface.[9,10] The electron affinity of ZnO is about 4.2 eV, which is larger than that of most common conjugated organic molecules. Therefore, the formation of a type-II energy level alignment with ZnO accepting an electron from the excited organic component is expected[10–13,15] resulting in nonradiative deactivation.[9,10] Such configuration, detrimental when targeting light-emitting applications, holds for many other conventional inorganic semiconductors as well.[9,16,17] Indeed, it was shown in previous work that the photoluminescence (PL) of a spirobifluorenene derivative is substantially quenched when in contact with ZnO due to interfacial exciton dissociation.[10] The same situation is encountered in polyfluorene/GaN HIOS[14] hampering so far the exploitation of the full potential of this class of heterostructures in light-emitting applications. Here, we present an effective strategy based on a FRET cascade to overcome this loss channel and to achieve highly luminescent HIOS.

The HIOS studied in this work are composed of a ZnO/ZnMgO QW structure covered with a thin layer of LOPPs. The inorganic part is grown on *a*-plane sapphire substrates by radical source molecular beam epitaxy. Details on the ZnO epitaxy can be found elsewhere.[18] The 3.5-nm thick ZnO QW is placed on top of a 500-nm thick lower $Zn_{0.9}Mg_{0.1}O$ barrier layer. The upper $Zn_{0.9}Mg_{0.1}O$ barrier separating QW and organic layer is kept sufficiently thin (2 nm) to allow for efficient FRET. The HIOS are completed with a top organic layer grown by molecular beam deposition. The growth rate (0.1 nm/min) and layer thickness are determined by a quartz crystal microbalance. In case of organic blends, the composition is adjusted via the deposition rates of the molecular components. The area of the organic layer is defined by a shadow mask leaving always an uncapped QW structure as reference. Growth of organic and inorganic component is performed in ultra-high vacuum while the samples are transferred from the inorganic to the organic growth chamber under high-vacuum conditions. FRET and charge separation are evaluated by a combination of PL, PL excitation (PLE), and time-resolved PL spectroscopy while the energy level alignment at the LOPP/ZnO interface is derived from ultraviolet photoelectron spectroscopy (UPS).

Before discussing the QW-LOPP FRET, we characterize the isolated components of our HIOS on reference samples. The chemical structures of two representatives of the

a)sylke.blumstengel@physik.hu-berlin.de

LOPP family suited as FRET acceptor molecules for ZnO, ladder-type quarterphenyl (L4P) and a triply spiro-annulated derivative (L4P-Sp3), are depicted in the insets of Figs. 1(a) and 1(b), respectively. Absorption spectra of a thin L4P-Sp3 film and of L4P dispersed in a PMMA matrix are shown together with PL spectra of a ZnO QW recorded at low and room temperature in Fig. 1(c). Both molecules exhibit well-resolved vibronic features with the $S_{0,\nu=0} \rightarrow S_{1,\nu=0}$ transitions overlapping extensively with the room-temperature QW PL so that one essential condition for efficient excitonic FRET is ensured. The transition energies of the molecules can be fine-tuned through attachment of different substituents at the bridging carbon atoms. Spiro groups, as shown here, cause a red-shift of the absorption spectrum of some 10 meV. Furthermore, packing of the molecules in the solid state as well as the film-forming properties can be adjusted in this way. L4P readily crystallizes.[7] However, for vacuum deposition on ZnO, Volmer-Weber growth prevails as evident from the atomic force microscopy (AFM) image in Fig. 1(a). The resultant films are composed of separated three-dimensional islands and are not suited for use in HIOS. On the contrary, spiro-annulated LOPPs grow in a two-dimensional mode, consistent with their reduced tendency to crystallize. In particular, L4P-Sp3 forms homogeneous films with a very smooth surface morphology [Fig. 1(b)]. In addition, the extended spiro groups prevent close packing of the molecules; and hence, the solid-state absorption spectrum is very similar to that of the isolated molecules in solution. In view of these advantageous features, L4P-Sp3 is selected in the present study.

We first evaluate FRET in a L4P-Sp3/ZnO/ZnMgO HIOS. The experiments described in the following are performed at cryogenic temperatures ($T = 5$ K) better suited to disentangle the relevant transfer processes. The PLE spectra reported in Fig. 1(d) are recorded by setting the detection energies to the L4P-Sp3 PL transition at $E_{det} = 3.12$ eV [Fig. 2(b)] or to the QW PL ($E_{det} = 3.352$ eV). The PLE spectrum of the QW displays the exciton ground- and excited-state absorption features as well as the ZnMgO band edge ($E_{ex} > 3.55$ eV), the latter indicating efficient capture of photo-excited carriers by the QW. All these features are also present in the molecular PLE demonstrating unambiguously exciton transfer from the ZnO QW to L4P-Sp3. PL transients are obtained by time-correlated single-photon counting using a mode-locked frequency-doubled fs-Ti:sapphire laser (5 W/cm^2, 76 MHz) as excitation source. The PL decay transient of the QW in absence of L4P-Sp3 is in good approximation single-exponentially with a time constant of $\tau_{QW} = 200$ ps. In the hybrid part covered with L4P-Sp3, the QW decay time shortens to $\tau^{h}_{QW} = 56$ ps verifying opening of an additional decay pathway for the QW excitons (Fig. 2(a)). Assuming that no parasitic losses on the QW side are introduced, we find a characteristic inorganic-organic FRET time of $\tau^{io}_{ET} = (1/\tau^{h}_{QW} - 1/\tau_{QW})^{-1} = 77$ ps and an efficiency of $\eta^{io}_{ET} = \tau^{h}_{QW}/\tau^{io}_{ET} = 0.72$, i.e., about three out of four excitons photogenerated in the QW are transferred to the L4P-Sp3 layer. However, inspection of the PL spectrum (Fig. 2(b)) shows that there is barely light produced by the organic layer. The quantum yield of L4P-Sp3 is sufficiently high in solid state and cannot serve as explanation. Consequently, there has to be an efficient pathway for the loss of excitation energy at the ZnMgO/L4P-Sp3 interface.

Valuable insights into the above issue are provided by UPS measurements, from which the energy level scheme depicted in Fig. 2(c) is derived. The experiment is performed at PM4 beamline at Bessy II (Germany) consisting of an

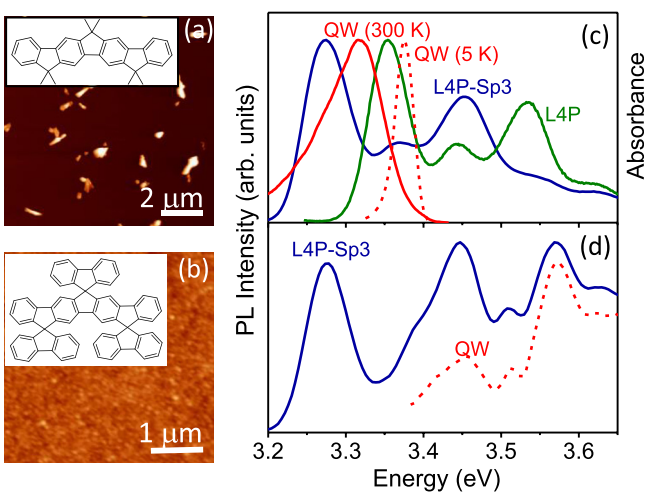

FIG. 1. AFM images of (a) L4P and (b) L4P-Sp3 deposited on ZnO. The nominal film thicknesses are 6 nm. The height scales of the images are (a) 300 nm and (b) 4 nm. The chemical structures of the molecules are depicted in the insets. (c) Room-temperature absorption spectra of L4P-Sp3 vacuum-deposited on Al_2O_3 (blue) and of L4P dispersed in a PMMA matrix (green). PL spectra of a ZnO/ZnMgO QW structure at temperatures of $T = 5$ K (red dashed) and $T = 300$ K (red solid). The excitation photon energy ($E_{ex} = 3.45$ eV) is below the ZnMgO band edge. (d) PLE spectra of a L4P-Sp3/ZnO/ZnMgO HIOS at $T = 5$ K. The L4P-Sp3 layer thickness is 4 nm. The detection energies are on the low-energy tail of the QW emission ($E_{det} = 3.352$ eV, red dashed) or on the Sp3-L4P PL transition at $E_{det} = 3.12$ eV (blue).

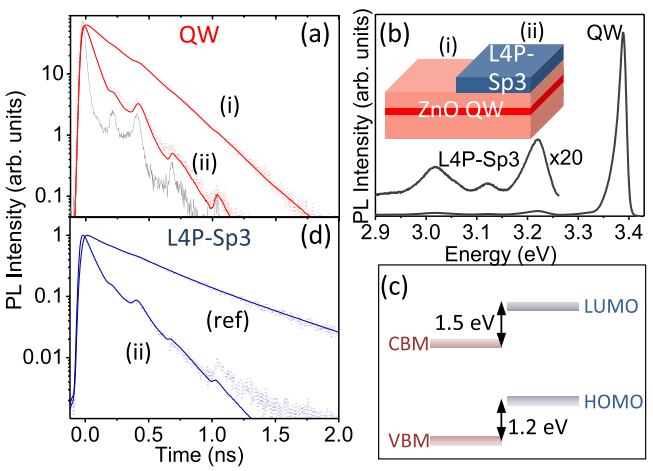

FIG. 2. FRET versus exciton dissociation in a L4P-Sp3/ZnO/ZnMgO HIOS. (a) PL transients of the ZnO QW in the uncapped (i) and hybrid part (ii) of the HIOS, see inset of (b). The solid lines are fits to the data obtained by convolution of a single- (i) and bi-exponential (ii) decay law, respectively, with the system response function shown in gray. The lifetime is defined as $\tau = \int tI(t)dt / \int I(t)dt$, where $I(t)$ is the decay transient. (b) PL spectrum of the hybrid region (ii). Note that the L4P-Sp3 emission is magnified by a factor of 20. Inset: sample layout. (c) Energy level alignment at the L4P-Sp3/ZnO interface derived from UPS and optical absorption measurements. (d) PL transients of L4P-Sp3 in HIOS region (ii) as well as for a reference sample (ref) deposited on sapphire. The fits to the data are performed as in (a). The excitation photon energy is $E_{ex} = 3.46$ eV and $T = 5$ K in all optical experiments.

interconnected sample preparation analysis UHV apparatus (base pressures 10^{-8} mbar and 10^{-10} mbar). Photoelectrons excited with 35 eV UV light are detected by a Scienta SES 100 spectrometer with ca. 200 meV energy resolution. Films of L4P-Sp3 are evaporated onto bulk ZnO single crystals (Tokyo Denpa) cleaned be repeated sputter/annealing cycles (1 kV, 20 mA, 40 min/400 °C). The energy offset between the valence band maximum (VBM) of ZnO and the highest occupied molecular orbital (HOMO) level of L4P-Sp3 deduced from the binding energy onsets amounts to 1.2 eV. The positions of the conduction band minimum (CBM) of ZnO and the lowest unoccupied molecular orbital (LUMO) level of L4P-Sp3 are estimated by adding the exciton binding energies [60 meV for ZnO and 450 meV for L4P-Sp3 (Ref. 19)] to the optical band gaps (3.3 eV for ZnO and 3.25 eV for L4P-Sp3) determined from the respective absorption spectra. The L4P-Sp3 LUMO is hence situated ≈1.5 eV above the ZnO CBM. As speculated above, a type-II interface is formed where the excitons undergo charge separation, with the electron in ZnO and the hole on the molecular side. In the present HIOS, the organic layer is in contact with the upper $Zn_{0.9}Mg_{0.1}O$ barrier with a band gap widened by only 0.3 eV relative to ZnO.[18] Therefore, the excitons initially collected in the QW and passed by FRET into L4P-Sp3 dissociate here as the energy gained by the electron transfer to the $Zn_{0.9}Mg_{0.1}O$ barrier still substantially exceeds their binding energy. The time-resolved molecular PL fully confirms the charge separation process [Fig. 2(d)]. The decay time of L4P-Sp3 in a reference layer is about $\tau_M = 500$ ps, whereas a shortening to $\tau_M^h \approx 95$ ps is found for the HIOS. The exciton quenching proceeds in two steps, namely, exciton diffusion towards the hybrid interface and subsequent dissociation of electron and hole. The 95-ps overall decay can thus be taken as an upper limit for the characteristic time of the charge separation process. As a consequence, a large fraction of the excitation energy is not converted into light. To be of use in light-emitting applications, exciton dissociation at the hybrid interface must therefore be prevented.

Tuning the energy levels into a type-I alignment, either by lowering the work function of ZnO via surface functionalization or by increasing the electron affinity of LOPPs by chemical modification, is difficult as the energy offsets are very large.[20,21] Note that also the use of molecules with substantially smaller HOMO-LUMO gaps will not circumvent the problem of competing charge separation. We performed experiments with the red-absorbing polymer poly((9,9-dioctylfluorene)-2,7-diyl-alt-[4,7-bis(3-hexylthien-5-yl)-2,1,3-benzothiadiazole]-2′,2″-diyl), which is even used as an acceptor in organic photovoltaics[22] and observed a substantial decrease of the PL lifetime from 1.1 ns to 315 ps when deposited on ZnO. We propose therefore a different strategy based on a fast and highly efficient FRET cascade: Following the primary FRET step starting at the ZnO QW, the excitation energy is funneled away from the hybrid interface by a secondary energy transfer step within the organic HIOS part before interfacial exciton dissociation can take place. As secondary acceptor and FRET partner for L4P-Sp3, a longer chain LOPP, namely, ladder-type sexiphenyl (L6P) is selected [inset of Fig. 3(a)].[6] The more extended π-electron

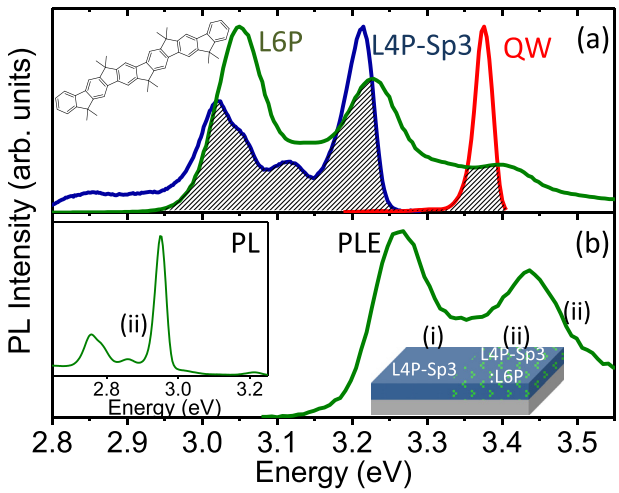

FIG. 3. FRET in a L4P-Sp3:L6P blend. (a) Spectral overlap between the absorption spectrum of L6P dispersed in PMMA (green) with the emission of L4P-Sp3 (blue) and the ZnO QW (red). The inset shows the structure of L6P. (b) PLE spectrum of a L4P-Sp3:L6P blend recorded at the $S_{1,\nu=0} \rightarrow S_{0,\nu=1}$ PL transition of L6P ($E_{det} = 2.755$ eV). The insets show the corresponding PL spectrum and the sample layout ($T = 5$ K in all measurements).

system of L6P shifts its $S_0 \rightarrow S_1$ absorption in resonance with the L4P-Sp3 emission, as demonstrated in Fig. 3(a). Furthermore, there is also spectral overlap between the $S_{0,\nu=0} \rightarrow S_{1,\nu=2}$ transition and ZnO so that direct energy transfer from the QW to L6P is in principle also possible. The FRET process within the organic layer is elucidated in blends obtained by co-evaporation of L4P-Sp3 and L6P on an inert substrate (Al_2O_3). A L6P fraction of 10% is low enough for avoiding phase separation, but sufficient for adequate FRET rates. The PL spectrum of the blend is indeed dominated by the L6P emission, while the signal from L4P-Sp3 is almost entirely quenched due to the presence of the acceptor molecules [inset Fig. 3(b)]. PLE data corroborate highly efficient FRET within the organic blend: The spectrum recorded at the vibronic $S_{1,\nu=0} \rightarrow S_{0,\nu=1}$ PL feature of L6P reproduces exactly the absorption spectrum of L4P-Sp3 (Fig. 3(b)). The PL decay of L4P-Sp3 in the blend can hardly be resolved by our photon counting setup providing an upper estimate of the time constant of the organic-organic FRET $\tau_{ET}^{oo} < 30$ ps at the present L4P-Sp3/L6P mixing ratio and a lower estimate of the efficiency $\eta_{ET}^{oo} > 0.9$. The decay time observed for L6P (curve not shown) is $\tau_{L6P} \approx 440$ ps.

Competition between the FRET cascade and interfacial exciton dissociation is studied on a HIOS composed of a ZnO/ZnMgO QW covered by a layer of a L4P-Sp3/L6P blend. To avoid interaction between ZnO and L6P, a 0.5-nm thick interlayer of pure L4P-Sp3 is introduced. The thickness of the blended layer is 3.5 nm so that the total width of the organic part is the same as in the "non-cascade" HIOS of Figs. 1(d) and 2. Indeed, in the "cascade" HIOS, prominent molecular emission of L6P arises [Fig. 4(a)]. The energy of the pump photons is chosen such that direct excitation of L6P is negligible. Details on the cascade process are attained from time-resolved PL measurements. First, the QW PL transients in the hybrid and reference part of the "cascade" HIOS depicted in Fig. 4(b) provide practically the same transfer time $\tau_{ET}^{io} = 65$ ps and efficiency $\eta_{ET}^{io} = 0.77$ as for the non-cascaded version in the sole L4P-Sp3 HIOS. That is,

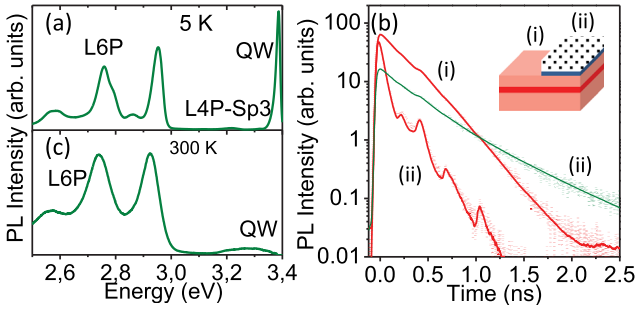

FIG. 4. Cascade FRET in a L6P:L4P-Sp3/ZnO/ZnMgO HIOS: (a) PL spectrum at $T = 5$ K. (b) PL transients ($T = 5$ K) of the ZnO QW (red) in the reference (i) and in the hybrid part (ii) as well as of L6P (green). The solid lines are fits to the data as described in Fig. 2. Inset: sample layout. (c) PL of the hybrid part (ii) of the cascade HIOS at 300 K. The excitation energy is $E_{ex} = 3.46$ eV.

the first step of the cascade is not modified. Second, the donor role of L4P-Sp3 in the next cascade step is verified by a further shortening of its decay time, now clearly below the 30-ps time-resolution. Third, in marked contrast to L4P-Sp3 in the single-stepped FRET, the PL decay time of L6P in the HIOS ($\tau_M^h \approx 400$ ps) is nearly identical to that of the blend on an inert substrate. All these observations imply that the excitation energy is effectively funneled away from the interface. The recovery of the molecular emission (R_{EM}) is measured by the ratio of the (spectrally integrated) yield of L6P in the "cascade" HIOS versus that of L4P-Sp3 in the "non-cascade" sample. As the inorganic-organic FRET is almost identical, the experimental ratio $R_{EM} \approx 10$ can be inferred by scaling the yield in both samples relative to that of the QW emission. Theoretically, denoting by σ_{L6P} and $\sigma_{L4P\text{-}Sp3}$, the radiative efficiency of the molecules in the respective HIOS, it holds $R_{EM} = \eta_{ET}^{oo}\sigma_{L6P}/\sigma_{L4P\text{-}Sp3}$. The radiative efficiency is $\sigma_M = \tau_M^h/\tau_M^{rad}$, where the total molecular lifetime τ_M^h is directly measured [95 ps (L4P-Sp3), 400 ps (L6P)], while the ratio of the radiative lifetimes can be quantified by comparing the molecular extinction coefficients providing $\tau_{L4P\text{-}Sp3}^{rad}/\tau_{L6P}^{rad} \approx 2$ and, finally, $R_{EM} \approx 8\,\eta_{ET}^{oo}$. This confirms the above estimate of $\eta_{ET}^{oo} \approx 1$ and demonstrates that FRET from L4P-Sp3 to L6P outpaces almost entirely the quenching of L4P-Sp3 excitons at the hybrid interface.

Cascade FRET persists up to room temperature as testified by the same set of measurements used above. The primary transfer from the QW to the L4P-Sp3 stays reasonably efficient ($\eta_{ET}^{io} = 0.32$) and the L6P emission is bright (Fig. 4(c)). These findings are remarkable as, generally, the quantum yield of inorganic QW structures declines at higher temperatures. Nonradiative recombination processes are thermally activated, while the radiative lifetime of the excitons becomes intrinsically longer.[23,24] The PL yield of the present ZnO/ZnMgO QWs drops roughly by a factor of 10 from $T = 5$ to 300 K. The FRET contribution from the QW excitons to the total L6P emission is measured under the present excitation conditions by the ratio $\eta_{ET}^{io}A_{QW}/[\eta_{ET}^{io}A_{QW} + A_{L4P\text{-}Sp3}] = 0.3$, where $A_{L4P\text{-}Sp3} = 0.07$ and $A_{QW} = 0.1$ are the fractions of photons absorbed in the L4P-Sp3 layer and the QW, respectively. Therefore, a substantial part of QW excitons otherwise lost by nonradiative recombination is recovered by FRET for light emission.

In conclusion, LOPPs are well suited FRET partners for ZnO. Charge separation caused by an unfavorable interfacial energy level alignment can be surpassed by cascade FRET where the second step takes place within a blend of suitably adjusted organic components. The resulting cascade does not noticeably reduce the total FRET efficiency. At room temperature, about one third of the excitons primarily excited in the QW are passed to the LOPP and emit light, whereas maximally one tenth would radiatively recombine in the sole QW. Hybrid FRET can thus effectively bypass non-radiative recombination. FRET-based hybrid light emitters are thus promising in terms of power consumption. Cascade FRET to suited acceptor molecules can furthermore be used for efficient color conversion or white light generation.[25] The HIOS presented in this work are not yet optimized and further improvements can be achieved by minimizing the FRET distance or optimizing the molecular packing.

Financial support of the Deutsche Forschungsgemeinschaft (SFB 951) is acknowledged.

[1]S. Blumstengel, S. Sadofev, C. Xu, J. Puls, and F. Henneberger, Phys. Rev. Lett. **97**, 237401 (2006).
[2]S. Blumstengel, S. Sadofev, and F. Henneberger, New J. Phys. **10**, 065010 (2008).
[3]J. J. Rindermann, G. Pozina, B. Monemar, L. Hultman, H. Amano, and P. G. Lagoudakis, Phys. Rev. Lett. **107**, 236805 (2005).
[4]G. Itskos, G. Heliotis, P. G. Lagoudakis, J. Lupton, N. P. Barradas, E. Alves, S. Pereira, I. M. Watson, M. D. Dawson, J. Feldmann, R. Murray, and D. D. C. Bradley, Phys. Rev. B **76**, 035344 (2007).
[5]S. Chanyawadee, P. G. Lagoudakis, R. T. Harley, D. G. Lidzey, and M. Henini, Phys. Rev. B **77**, 193402 (2008).
[6]B. Kobin, L. Grubert, S. Blumstengel, F. Henneberger, and S. Hecht, J. Mater. Chem. **22**, 4383 (2012).
[7]B. Kobin, L. Grubert, S. Mebs, B. Braun, and S. Hecht, Isr. J. Chem. **54**, 789 (2014).
[8]U. Scherf and K. Müllen, Makromol. Chem., Rapid Commun. **12**, 489 (1991).
[9]A. A. Lutich, G. Jiang, A. S. Susha, A. L. Rogach, F. D. Stefani, and J. Feldmann, Nano Lett. **9**, 2636 (2009).
[10]S. Blumstengel, S. Sadofev, C. Xu, J. Puls, R. L. Johnson, H. Glowatzki, N. Koch, and F. Henneberger, Phys. Rev. B **77**, 085323 (2008).
[11]S. Blumstengel, H. Glowatzki, S. Sadofev, N. Koch, S. Kowarik, J. P. Rabe, and F. Henneberger, Phys. Chem. Chem. Phys. **12**, 11642 (2010).
[12]S. Rangan, S. Katalinic, R. Thorpe, R. A. Bartynski, J. Rochford, and E. Galoppini, J. Phys. Chem. C **114**, 1139 (2010).
[13]R. J. Davis, M. T. Lloyd, S. R. Ferreira, M. J. Bruzek, S. E. Watkins, L. Lindell, P. Sehati, M. Fahlman, J. E. Anthony, and J. W. P. Hsux, J. Mater. Chem. **21**, 1721 (2011).
[14]G. Itskos, X. Xristodoulou, E. Iliopoulos, S. Ladas, S. Kennou, M. Neophytou, and S. Choulis, Appl. Phys. Lett. **102**, 063303 (2013).
[15]S. H. Park, H. J. Kim, M.-H. Cho, Y. Yi, S. W. Cho, J. Yang, and H. Kim, Appl. Phys. Lett. **98**, 082111 (2011).
[16]S. Blumstengel, N. Koch, S. Duhm, H. Glowatzky, R. L. Johnson, C. Xu, A. Yassar, J. P. Rabe, and F. Henneberger, Phys. Rev. B **73**, 165323 (2006).
[17]H. Kim, Z.-L. Guan, Q. Sun, A. Kahn, J. Han, and A. Nurmikko, J. Appl. Phys. **107**, 113707 (2010).
[18]S. Sadofev, S. Blumstengel, J. Cui, J. Puls, S. Rogaschewski, P. Schäfer, Yu. G. Sadofyev, and F. Henneberger, Appl. Phys. Lett. **87**, 091903 (2005).
[19]M. Kemerink, S. F. Alvarado, P. Muller, P. M. Koenraad, H. W. M. Salemink, J. H. Wolter, and R. A. J. Janssen, Phys. Rev. B **70**, 045202 (2004).
[20]N. Kedem, S. Blumstengel, F. Henneberger, H. Cohen, G. Hodes, and D. Cahen, Phys. Chem. Chem. Phys. **16**, 8310 (2014).
[21]O. T. Hofmann, J.-C. Deinert, Y. Xu, P. Rinke, J. Sthler, M. Wolf, and M. Scheffler, J. Chem. Phys. **139**, 174701 (2013).

[22]C. R. McNeill, A. Abrusci, J. Zaumseil, R. Wilson, M. J. McKiernan, J. H. Burroughes, J. J. M. Halls, N. C. Greenham, and R. H. Friend, Appl. Phys. Lett. **90**, 193506 (2007).
[23]J. Feldmann, G. Peter, E. O. Göbel, P. Dawson, K. Moore, C. Foxon, and R. J. Elliott, Phys. Rev. Lett. **59**, 2337 (1987).
[24]A. Esser, E. Runge, R. Zimmermann, and W. Langbein, Phys. Rev. B **62**, 8232 (2000).
[25]G. Itskos, C. R. Belton, G. Heliotis, I. M. Watson, M. D. Dawson, R. Murray, and D. D. C. Bradley, Nanotechnology **20**, 275207 (2009).